

Random matrix theory and classical statistical mechanics: Spin models

H. Meyer* and J.-C. Anglès d'Auriac†

Centre de Recherches sur les Très Basses Températures, Boîte Postale 166, 38042 Grenoble, France

(Received 17 December 1996)

We present a statistical analysis of spectra of transfer matrices of classical lattice spin models; this continues the work on the eight-vertex model of the preceding paper [H. Meyer, J.-C. Anglès d'Auriac, and J.-M. Maillard, *Phys. Rev. E* **55**, 5261 (1997)]. We show that the statistical properties of these spectra can serve as a criterion of integrability. It also provides an operational numerical method to locate integrable varieties. In particular, we distinguish the notions of integrability and criticality, considering the two examples of the three-dimensional Ising critical point and the two-dimensional three-state Potts critical point. For complex spectra, which appear frequently in the context of transfer matrices, we show that the notion of independence of eigenvalues for integrable models still holds. [S1063-651X(97)02806-7]

PACS number(s): 05.50.+q, 05.20.-y, 05.45.+b

I. INTRODUCTION

Random matrix theory (RMT) has been applied in surprisingly many fields of physics and mathematics. In a recent paper [1] we proposed its application to transfer matrices of lattice models in classical statistical mechanics. In a preceding paper [2], referred to hereafter as paper I, we gave the details of this RMT analysis applied to the general eight-vertex model. We showed numerically that the integrability of the model can be seen on the statistical properties of the entire spectrum of transfer matrices of vertex models. Using this as a criterion for integrability, we located all the known integrable varieties in the parameter space. In this paper we continue this work with the study of spin models. Many aspects were already presented in paper I, so we will recall below only the basic ideas of the RMT analysis with emphasis on the points which are specific to spin models.

An important area of application of RMT is the characterization of chaos [3,4]. One can describe the fluctuations of energy spectra of chaotic systems with some ensembles of RMT, while the spectra of regular systems show the characteristics of independent numbers (Poissonian ensemble). In classical (Hamiltonian) mechanics, the notions of regular and chaotic dynamics coincide with the notions of integrability and nonintegrability. But in quantum mechanics the notions of chaos and integrability are less precise; one nowadays adopts the criterion of RMT as a definition of quantum chaos. For models of quantum statistical mechanics one can adopt a definition of integrability related to the Bethe ansatz: an integrable system is a system for which a complete set of eigenstates having the Bethe ansatz form exists. For a classical statistical mechanics model, the notion of integrability is generally related to the Yang-Baxter equations. For example, solving the Yang-Baxter equations for the symmetric eight-vertex model (also called the Baxter model) allows one to build a one-parameter family of commuting transfer ma-

trices, and finally to compute the free energy of the model [5,6]. The spin version of the Yang-Baxter equations are the star-triangle equations introduced earlier [7,6]. Solving these star-triangle equations also allows one to construct an infinite family of commuting transfer matrices. We note that a vertex model can be turned into a spin model with many-spin interactions (see, for example, Ref. [8]). In this paper, we treat spin models including only two-spin interactions, possibly coupled to an external field, and by integrable we mean Yang-Baxter integrable as well as star-triangle integrable.

The spectrum of an integrable system, after a suitable treatment, has been shown to have many properties of a set of random *independent* numbers (Poissonian behavior), while the spectrum of a chaotic system is described quite accurately by the spectrum of matrices of statistical ensembles. The choice of the proper ensemble depends on very general symmetry properties of the model under consideration. For a time reversal symmetric model this ensemble is the Gaussian orthogonal ensemble (GOE) [9,4]. This classification scheme has been applied successfully to quantum spin models in one dimension [10,11] and on two-dimensional lattices [12–15].

For a classical lattice spin model, the energy spectrum is usually very simple. (For an Ising model this spectrum contains all the possible numbers of violated bonds, i.e., the set of integers $[0, N_b]$, where N_b is the number of bonds; the physical properties of the model are contained in the degeneracies, and its statistical properties were studied in Ref. [13].) Therefore the analysis has to be performed on another quantity. The transfer matrix is such an operator (related to the Hamiltonian) which describes completely the thermodynamic properties of a system including the size effects [16], and we will perform the RMT analysis on its spectrum. It was already shown in paper I and in [1] that the notion of Yang-Baxter integrability coincides with a Poissonian spectrum, and that nonintegrable spectra are described by GOE matrix spectra. To perform this RMT analysis in its usual form, one needs to deal with a real spectrum. For spin models, and when the interactions are nonchiral (symmetric), this can be achieved using the so-called row-to-row (or layer-to-layer in higher dimension) transfer matrix, as explained below. We also studied the spectra in the nonphysical regime where the Boltzmann weights are not positive. Indeed, most of the analytical results concern varieties in the entire param-

*Present address: FB10 Theoretische Tieftemperaturphysik, Gerhard-Mercator-Universität, 47048 Duisburg, Germany. Electronic address: hmeyer@crbtb.polycnrs-gre.fr

†Electronic address: dauriac@crbtb.polycnrs-gre.fr

eter space including the region where the Boltzmann weights are negative. In this region, even row-to-row transfer matrices can have complex eigenvalues. The necessary changes in the analysis will be discussed briefly.

The plan of this paper is the following. In Sec. II we recall the numerical methods of the RMT analysis with a special emphasis on the specificity of the spin models we investigate. In Sec. III we present the numerical results, successively, of the two-dimensional Ising model in the absence of magnetic field (a paradigm of an integrable system), the same two-dimensional Ising model in a magnetic field, the three-dimensional Ising model (a paradigm of a nonintegrable system), and the three-state Potts model. The three-state Potts model provides an example of a point which is integrable and critical at the same time. By contrast, the three-dimensional Ising model provides a nonintegrable, but critical, point. Finally, we investigate a nonphysical self-dual point of the three-state Potts model. This is an attempt to study complex spectra in the context of this statistical analysis of transfer matrices. We conclude in Sec. IV with a discussion.

II. NUMERICAL METHODS OF RMT IN THE CONTEXT OF SPIN MODELS

The machinery of random matrix theory was explained in details in paper I. It consists of five distinct steps: (i) choose a representation basis for the operator and construct the corresponding matrix; (ii) find the parameter-independent stable subspaces and the matrices representing the operator in each of these subspaces; (iii) diagonalize each matrix; (iv) ‘‘unfold’’ each spectrum; and (v) compute all the spectral quantities. In this section, we briefly discuss these five points, and give details which are specific to the spin models studied in this paper.

(i) We use the transfer matrix formalism, where the lattice is built up adding identical ‘‘generating sublattices.’’ These generating sublattices can be rows for two-dimensional models or rectangular layers for three-dimensional lattices. For spin models, it is well known that this transfer matrix can be factorized as

$$\begin{aligned} T(K_1, K_2, \dots, K_n) \\ = V^{1/2}(K_2, \dots, K_n) H(K_1) V^{1/2}(K_2, \dots, K_n) , \end{aligned} \quad (1)$$

where H contains the interactions between two generating sublattices and V contains the interactions inside a generating sublattice; V is usually a diagonal matrix. K_i are the coupling constants in the different directions; we assign direction 1 to be the direction in which the lattice grows. For each case we study in this paper, the precise form of V and H are given in the corresponding section. In form (1), the transfer matrix is a symmetric matrix if the interaction between the two layers and thus the matrix H is symmetric. If the Boltzmann weights are real positive, the entries of the transfer matrix are also real positive. In this case of a real and symmetric (transfer) matrix the spectrum is real, so that the methods for the statistical analysis presented in paper I apply.

(ii) To find the parameter-independent subspaces one needs to know the symmetries of the generating sublattices. For the transfer matrix of a d -dimensional hypercubic lattice these generating sublattices are $(d-1)$ -dimensional lattices. For the square lattice, the generating sublattice is a periodic chain. As explained in paper I the symmetry group is the dihedral group \mathcal{D}_N . For a three-dimensional cubic lattice we use a square lattice as the generating sublattice. For an isotropic square lattice the automorphy group has been detailed in [15] (with emphasis on the atypical case $N=4$). It is a large group which leads to consequent size reduction (see Sec. IIIC). In addition to these space symmetries there is a ‘‘color symmetry’’ when no field is applied. This symmetry reflects the fact that the Hamiltonian is invariant under a permutation of the possible values of the spin variables (i.e., spin reversal symmetry for the Ising model). For a q -state model, this is an S_q symmetry; in this paper we work with $q=2$ and 3. This color symmetry commutes with the space symmetries.

(iii) The diagonalization of the blocks is done numerically using standard procedures of the LAPACK library. We note that the block diagonalization of step (ii) requires more numerical effort (CPU time) than the diagonalization of one block.

(iv) The unfolding procedure is the same as the procedure detailed in paper I. It produces the unfolded eigenvalues ϵ from the raw eigenvalues λ . The spectra of spin and vertex models are quite similar. However, we also have analyzed *complex* spectra. In that case the eigenvalues are seen as points in the plane (and not on a line) the local density of which has to be made constant. To unfold complex spectra we follow the procedure described in Chap. 8.6 of Ref. [4].

(v) The spectral analysis is performed on the same quantities as in paper I. These are the level spacing distribution $P(s)$ of the differences between two consecutive unfolded eigenvalues $s_i = \epsilon_{i+1} - \epsilon_i$. For a nonintegrable model, the eigenvalue spacing distribution is very close to the Wigner surmise for the GOE,

$$P(s \equiv \lambda_{i+1} - \lambda_i) = \frac{\pi}{2} s \exp(-\pi s^2/4) , \quad (2)$$

in contrast with the exponential $P(s) = e^{-s}$ for a set of independent eigenvalues for an integrable model. The spectral rigidity is

$$\Delta_3(L) = \left\langle \frac{1}{L} \min_{a,b} \int_{\alpha-L/2}^{\alpha+L/2} [N_u(\epsilon) - a\epsilon - b]^2 d\epsilon \right\rangle_{\alpha} , \quad (3)$$

where $N_u(\epsilon) \equiv \sum_i \theta(\epsilon - \epsilon_i)$ is the integrated density of unfolded eigenvalues and $\langle \rangle_{\alpha}$ denotes an average over α . Another quantity of interest is the number variance $\Sigma^2(L)$, defined as the variance of the number of unfolded eigenvalues in an interval of length L ,

$$\Sigma^2(L) = \left\langle \left[N_u\left(\epsilon + \frac{L}{2}\right) - N_u\left(\epsilon - \frac{L}{2}\right) - L \right]^2 \right\rangle_{\epsilon} , \quad (4)$$

where the brackets denote an averaging over ϵ . The expected behavior in the limiting cases of independent numbers and GOE spectra was recalled in paper I; for more details see, for example, Refs. [9,4].

We also recall the parametrized probability distribution we use to interpolate between the Poisson law and the Wigner law (Ref. [9], Chap. 16.8):

$$P_\beta(s) = c(1 + \beta) s^\beta \exp(-cs^{\beta+1}), \quad (5)$$

with $c = (\Gamma[(\beta+2)/(\beta+1)])^{1+\beta}$. The interpolation parameter β proved itself to be a useful indicator for the localization of integrable varieties [2]. There should be no confusion of this parameter β with the inverse temperature $1/k_B T$ [17].

III. RESULTS OF THE RMT ANALYSIS

A. Two-dimensional Ising model without magnetic field

We start our analysis with the two-dimensional Ising model, which is well known to be integrable in the absence of a magnetic field [18]. To work with symmetric matrices we use the row-to-row transfer matrix. For a rectangular $N \times M$ lattice with periodic boundary conditions the (reduced) Hamiltonian reads

$$\beta \mathcal{H}_{N,M}^0(K_1, K_2) = - \sum_{i=0}^{N-1} \sum_{j=0}^{M-1} \sigma_{i,j} (K_1 \sigma_{i,j+1} + K_2 \sigma_{i+1,j}), \quad (6)$$

where β is the inverse temperature, and K_1 and K_2 are the coupling constants in the two directions divided by the temperature. The partition function is

$$Z_{N,M}(K_1, K_2) = \sum \exp[\beta \mathcal{H}_{N,M}^0(K_1, K_2)] = \text{Tr} T_N^M(K_1, K_2), \quad (7)$$

where the row-to-row transfer matrix $T_N(K_1, K_2)$ is given by

$$T_N(K_1, K_2) = V(K_2) H(K_1). \quad (8)$$

The matrix $V(K_2)$ is a $2^N \times 2^N$ diagonal matrix with entries

$$[V(K_2)]_{\alpha, \alpha} = \prod_{i=0}^{N-1} w_2^{\alpha_i \alpha_{i+1}}, \quad (9)$$

where $\alpha_i = \pm 1$, according to the i th digit of the binary representation of α and $w_2 = e^{K_2}$. The matrix $H(K_1)$ is a symmetric matrix

$$H(K_1) = h(K_1)^{\otimes N}, \quad h(K_1) = \begin{pmatrix} w_1 & w_1^{-1} \\ w_1^{-1} & w_1 \end{pmatrix}, \quad (10)$$

with $w_1 = e^{K_1}$. Note that K_1 and K_2 do not play the same role here. If all the Boltzmann weights are real and positive, and using the circular property of the trace, $T_N(K_1, K_2)$ can be replaced by a similar matrix

$$T_N(K_1, K_2) = V^{1/2}(K_2) H(K_1) V^{1/2}(K_2). \quad (11)$$

It is clear that $T_N(K_1, K_2)$ is symmetric and therefore has a real spectrum. This spectrum has been completely worked out for even size N in [19]. From the explicit form of the eigenvalues it is easy to check that the entire spectrum is invariant by negating the Boltzmann weights w_i , and we can restrict ourselves to the physical case $w_i > 0$.

In Ref. [19] it is shown that the problem of diagonalizing $T_N(K_1, K_2)$ can be turned into a problem of free fermions. One has

$$T_N(K_1, K_2) = (2 \sinh 2K_1)^{N/2} \exp \left(- \sum_{q=0}^{N-1} \epsilon_q \left(\xi_q^+ \xi_q - \frac{1}{2} \right) \right), \quad (12)$$

where ξ_q are fermionic operators. The dispersion relation $\epsilon_q(K_1, K_2)$ is a cosine, and its detailed form depends on the parity of the number of ξ particles. Therefore, fixing the ‘‘quantum number’’ q_i , where q_i is the momentum of the i th ξ particle, *completely* determines an eigenvalue and an eigenstate of the transfer matrix. However, instead of using the complete set of quantum numbers, we take only into account the quantum numbers which correspond to parameter-independent symmetries. As mentioned in Sec. II, the space symmetries of $T_N(K_1, K_2)$ form a group isomorphic to the dihedral group $\mathcal{D}_N = Z_N \rtimes Z_2$ (\rtimes is the semidirect product), and in the absence of a magnetic field the spin reversal symmetry induces an extra Z_2 symmetry which commutes with \mathcal{D}_N . Using the projectors independent of K_1 and K_2 onto the corresponding invariant subspaces, the transfer matrix is block diagonalized. The dimensions of the blocks are given in Table I. We note that using these projectors leaves a few degeneracies inside some blocks. We also note that some eigenvalues are independent of the value of K_2 . In Appendix A all these $2^{N/2+1}$ K_2 -independent eigenvalues occurring only when the size N is a multiple of four, are determined analytically.

Having discarded the degenerate states and the K_2 -independent states in each representation one can perform the RMT analysis. Figure 1 shows the level spacing distribution for $w_1 = w_2 = 1.4$ of the representation labeled $R=4, C=0$ of $N=16$ (see Table I). One finds roughly an exponential distribution which is expected for an integrable model. Our explanation for the deviation from the exponential is the following: for an integrable system we do not sort the states according to all their ‘‘quantum numbers’’ (doing that will leave us with blocks of size 1). We therefore treat together eigenvalues belonging to states having different symmetries, but these states are only approximately independent. We also performed the same numerical analysis on *all* eigenvalues computed with formula (A1) and the result is even worse. This result is characteristic of the free-fermion nature of the problem (note that the parameter β has been found always negative on the free-fermion variety of the eight-vertex model [2]). The same form of the spacing distribution is found for any value of the Boltzmann weights, even for negative Boltzmann weights. However, if one of the Boltzmann weight is ‘‘too large’’ or ‘‘too small,’’ some entries of the transfer matrix become huge, and this leads to numerical instabilities in the diagonalization. On the other hand, if the Boltzmann weights are ‘‘too close’’ to unity (decoupling limit) many eigenvalues are almost degenerate, which leads to difficulties in the unfolding procedure. We note finally that the critical point does not manifest itself in any manner on the spacing distribution nor on the spectral rigidity Δ_3 .

TABLE I. Two-dimensional Ising model: the symmetries of a periodic chain combined with the Z_2 color symmetry. The dimensions a_R and degeneracies l_R of the invariant subspaces for $N=14$ and 16. R is an arbitrary label of the representations of the dihedral group, $\exp(ik)$ and λ are the eigenvalues of the corresponding translation and reflection operators (* means that the corresponding representation is not stable under the action of the reflection operator). The column $a_{R,C=0}$ ($a_{R,C=1}$) refers to states which are even (odd) under spin reversal. The column a_R is the sum of the two preceding for the case where a magnetic field breaks the spin reversal symmetry.

Ising model on a periodic square lattice						
$N=14, \dim=16\ 384$						
R	k	λ	l_R	$a_{R,C=0}$	$a_{R,C=1}$	a_R
0	0	1	1	362	325	687
1	π	-1	1	288	325	613
2	0	-1	1	234	261	495
3	π	1	1	288	261	549
4	$2\pi/7$	*	2	594	585	1179
5	$4\pi/7$	*	2	594	585	1179
6	$6\pi/7$	*	2	594	585	1179
7	$\pi/7$	*	2	576	585	1161
8	$3\pi/7$	*	2	576	585	1161
9	$5\pi/7$	*	2	576	585	1161

$N=16, \dim=65\ 536$						
R	k	λ	l_R	$a_{R,C=0}$	$a_{R,C=1}$	a_R
0	0	1	1	1162	1088	2250
1	π	-1	1	1033	1088	2121
2	0	-1	1	906	960	1866
3	π	1	1	1033	960	1993
4	$\pi/2$	*	2	2065	2048	4113
5	$\pi/4$	*	2	2062	2048	4110
6	$3\pi/4$	*	2	2062	2048	4110
7	$\pi/8$	*	2	2032	2048	4080
8	$7\pi/8$	*	2	2032	2048	4080
9	$5\pi/8$	*	2	2032	2048	4080
10	$3\pi/8$	*	2	2032	2048	4080

B. Two-dimensional Ising model in a magnetic field

We now investigate the case where a magnetic field is turned on. The Hamiltonian becomes

$$\beta\mathcal{H}_{N,M}(K_1, K_2) = \beta\mathcal{H}_{N,M}^0(K_1, K_2) - K \sum_{i=0}^{N-1} \sum_{j=0}^{M-1} \sigma_{i,j}, \quad (13)$$

K being the field times the inverse temperature, and the transfer matrix reads

$$T_N(K_1, K_2, K) = [V(K_2)B(K)]^{1/2} H(K_1) [V(K_2)B(K)]^{1/2}, \quad (14)$$

where H and V are the same matrices as defined by Eqs. (10) and (9) and $B(K)$ is a diagonal matrix with entries

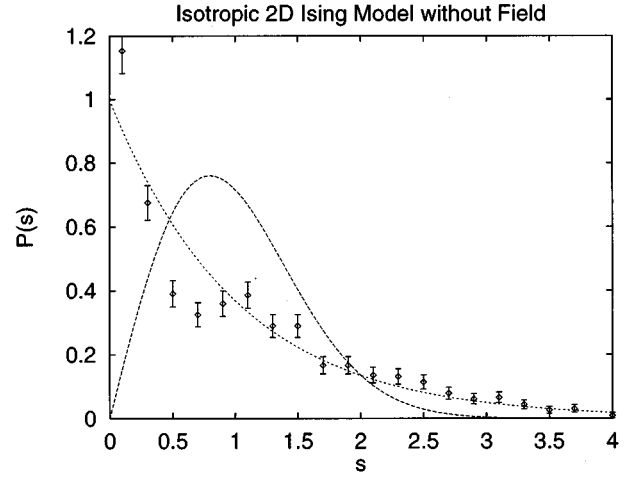


FIG. 1. The eigenvalue spacing distribution for the row-to-row transfer matrix of the isotropic two-dimensional Ising model. The linear size is $N=16$, and the Boltzmann weight is $w_1=w_2=1.4$. The spacings are taken in the largest representation. The average is over 1400 observations.

$$[B(K)]_{\alpha,\alpha} = \prod_{i=0}^{N-1} w^{\alpha_i}, \quad (15)$$

where $\alpha_i = \pm 1$ according to the i th bit of the binary representation of α , and $w = e^K$. The spin reversal symmetry no longer holds.

It is known that this model is not Yang-Baxter integrable, and its partition function has not yet been summed up. In Fig. 2 we present the spacing distribution and the spectral rigidity for a typical large representation (labeled $R=4$ in Table I) for $L=14$. The temperature is $T=1.4$, and the magnetic field is $H=0.8$. The statistics is taken over 1100 spacings. The spacing distribution clearly coincides with the Wigner surmise. The agreement of the spectral rigidity Δ_3 and the number variance Σ^2 with same quantities computed for the GOE matrices is surprisingly good: it holds up to a value of $L=25$ for the spectral rigidity, and only up to $L=7$ for the number variance, a value much larger than for other models of statistical mechanics [2]. To appreciate how the magnetic field influences the spacing distribution, in Fig. 3 we plot the best fitted value β of the Brody distribution P_β , Eq. (5), as a function of the Boltzmann weight associated with the field. The behavior of β is unambiguous: the magnetic field induces a Wigner-type distribution of the spacing distribution. The drop of β is sharp as the magnetic field goes to zero. In Fig. 3 the negative value of the parameter β in zero field is due to the free-fermion nature of the two-dimensional Ising model in the absence of a magnetic field. We interpret the small width of the peak as a size effect, and we claim that in the thermodynamic limit β is strictly zero only for a zero magnetic field. This underlines the very singular nature of integrability. Probing the value of β in the physical region of the parameter space, we did not find any other integrable points than the points where the magnetic field is zero.

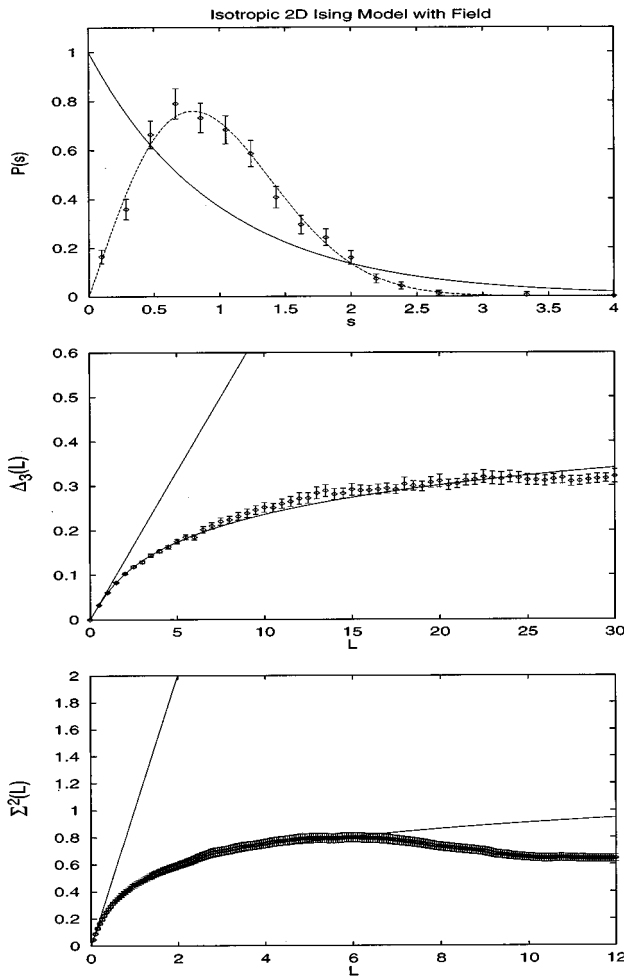


FIG. 2. The eigenvalue spacing distribution $P(s)$, the rigidity Δ_3 , and the number variance Σ^2 for the row-to-row transfer matrix of the isotropic two-dimensional Ising model in a field. The linear size is $N=14$, the temperature is $T=1.4$, and the magnetic field is $H=0.8$. The spacings are taken in the representation labeled $R=4$. The average is over 1100 observations.

C. Three-dimensional Ising model

We now investigate another archetypal case of nonintegrability in statistical mechanics: the three-dimensional Ising model. This model can still be mapped onto a fermion problem as in two dimensions, but in three dimensions the fermions are correlated [20], and the partition function cannot be summed up in a closed form.

We build the lattice by adding *square isotropic* layers. Let K_2 be the interaction in the two directions inside the layers and K_1 the interaction in the direction perpendicular to the layers (i.e., the cubic lattice is built in the direction of K_1). We again have $T_N(K_1, K_2) = V^{1/2}(K_2)H(K_1)V^{1/2}(K_2)$. The matrix $V(K_2)$ is a $2^{N^2} \times 2^{N^2}$ diagonal matrix with entries

$$[V(K_2)]_{\alpha, \alpha} = \prod_{i=0}^{N-1} \prod_{j=0}^{N-1} w_2^{\alpha_{i,j}(\alpha_{i,j+1} + \alpha_{i+1,j})}, \quad (16)$$

where $\alpha_{i,j} = \pm 1$ (the sums in the indices are taken modulo N). The matrix $H(K_1)$ is a symmetric matrix with entries

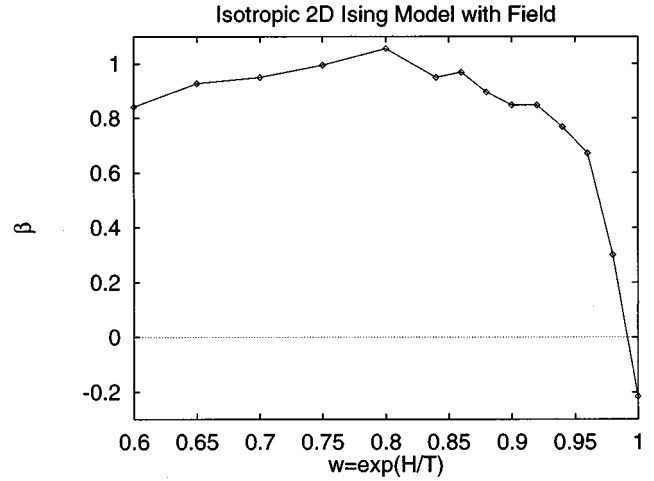


FIG. 3. The parameter β for the isotropic square lattice Ising model as a function of the Boltzmann weight $w = \exp(H/T)$ associated with the field. The other Boltzmann weights are kept constant $w_1 = w_2 = 1.6$ which determines the temperature as $T \approx 2.1$. Average over the representations $R=0$ and 4 for $N=14$ (approximately 1700 spacings).

$$[H(K_1)]_{\alpha, \beta} = \prod_{i,j=0}^{N-1} w_1^{\alpha_{i,j} \beta_{i,j}}. \quad (17)$$

We again need to project the transfer matrix into the parameter-independent invariant subspaces. Without magnetic field we still have the spin reversal symmetry, but the space group is more involved than for the two-dimensional model, since the automorphy group of a square lattice is larger than the automorphy group of a ring (see Sec. II). Using rectangular $N \times N'$ layers would have led to much simpler calculations, since the symmetry group would have been simply $\mathcal{D}_N \otimes \mathcal{D}_{N'}$. However, the size reduction of the matrix would have been less and consequently also the numerically accessible lattice sizes. It is worth noting at this point that the size effects are not controlled by the dimension of the subblocks of the transfer matrix, but by the size of the lattice. Moreover, we studied the particular case $N=4$ for which the generic symmetry group of the isotropic square lattice C_{4v} has to be replaced by a larger group (for the technical details, see [15]). In contrast with the two-dimensional case, projecting onto invariant subspaces lifts *all* degeneracies within each subblock (note that using the generic C_{4v} group would have left degeneracies inside some blocks). Table II shows the size of the invariant subspaces.

The results of the RMT analysis are presented in Fig. 4. The eigenvalue spacing distribution for the representations labeled $R=17$ and 18 in Table II are averaged together. After discarding some eigenvalues close to the edge of the spectrum, we are left with 2000 spacings. We observe that the level spacing distribution is very close to a Wigner distribution. Also, the spectral rigidity and the number variance are in agreement with the corresponding quantities of GOE matrices. We paid special attention to the critical point, since it is an example of a nonintegrable, nevertheless critical, point. No special behavior is found. This strongly suggests that the statistical properties of the eigenvalues of transfer

TABLE II. Three-dimensional Ising model: the symmetry of an isotropic square lattice with periodic boundary conditions combined with the Z_2 color symmetry. The notations are the same as in Table I.

Ising model on a periodic cubic lattice				
$N=4, \dim=65\,536$				
R	l_R	$a_{R,C=0}$	$a_{R,C=1}$	a_R
0	1	222	180	402
1	1	50	44	94
2	1	169	180	349
3	1	33	44	77
4	2	191	192	383
5	2	211	192	403
6	3	186	180	366
7	3	291	300	591
8	3	183	180	363
9	3	354	300	654
10	4	460	480	940
11	4	236	224	460
12	4	460	480	940
13	4	236	224	460
14	6	397	416	813
15	6	507	480	987
16	6	447	480	927
17	6	681	672	1353
18	8	668	672	1340
19	8	668	672	1340

matrices are governed by the status of the model with respect to integrability rather than to criticality.

To go from a two-dimensional model to a three-dimensional model, we recorded the value of β when the interaction w_1 in the third dimension is turned on continuously. Figure 5 summarizes the results: a vanishingly small coupling in the third direction induces level repulsion. It is

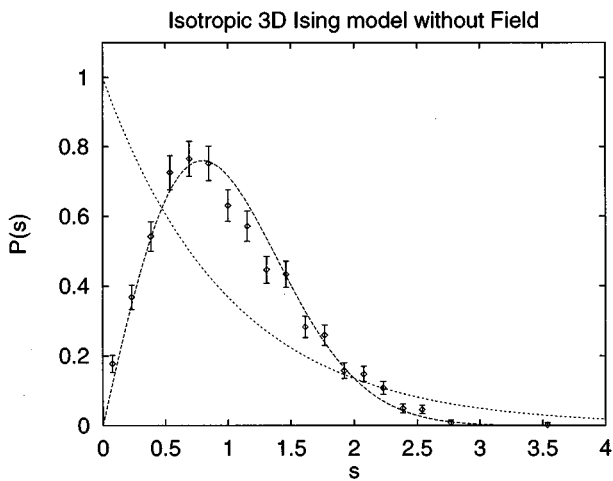


FIG. 4. The eigenvalue spacing distribution for the row-to-row transfer matrix of the isotropic three-dimensional Ising model at the critical point. The linear size is $N=4$. The spacings are averaged over the representations labeled 17 and 18. The average is over 2000 observations.

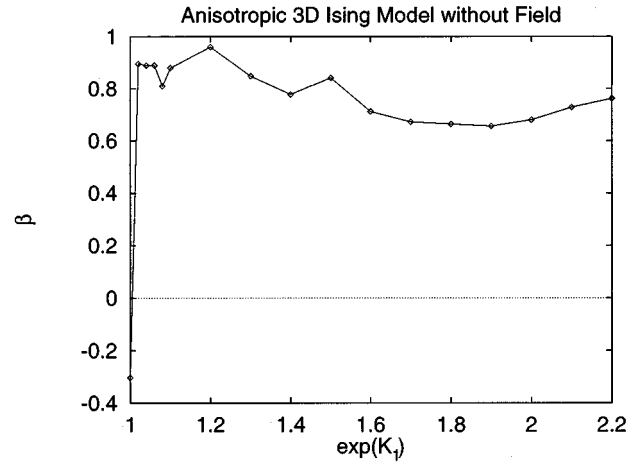


FIG. 5. The best fitted β parameter as a function of e^{K_1} for the anisotropic three-dimensional Ising model. The average runs over 2000 spacings. The point $e^{K_1}=1$ corresponds to a two-dimensional model.

remarkable that with such a small size $N=4$ we already have a very abrupt variation of β . This once again stresses the singular nature of integrability.

D. Three-state potts model on a square lattice

We now turn to the case of the Potts model (see Ref. [21], and references therein). This spin model is a generalization of the Ising model where the spins can take more than two values. The Hamiltonian is

$$\beta \mathcal{H}_{N,M}^0(K_1, K_2) = - \sum_{i=0}^{N-1} \sum_{j=0}^{M-1} [K_1 \delta(\sigma_{i,j}, \sigma_{i,j+1}) + K_2 \delta(\sigma_{i,j}, \sigma_{i+1,j})] , \quad (18)$$

where δ is a Kronecker symbol, β is the inverse temperature, K_1 and K_2 are the coupling constants divided by the temperature, and $\sigma \in Z_q$ can take q values. This has been investigated by many authors, but its full solution is still a challenge. Using a duality relation, one can localize a phase transition at the temperature $T_c = 1/\ln(1 + \sqrt{q})$ for any number q of states [22]. The model can be mapped onto a staggered six-vertex model, the parameters of which depend on K_1 , K_2 , and q [6]. This six-vertex model is in general not integrable, since there are two different sets of Boltzmann weights, one for each sublattice of the square lattice. However, for a special combination of the parameters the two sets of Boltzmann weights are the same and, consequently, the partition function of the model can be calculated. This line, where the partition function can be calculated, turns out to be the critical line. Here, in contrast with the three-dimensional Ising model, the two notions of integrability and criticality coincide.

We have numerically investigated the case of the three-state Potts model. For $q=3$ this model presents a second-order phase transition which is not of the same universality class as the transition of the Ising model. For the isotropic case the transition is given by $(e^K - 1)^2 = q = 3$. It would have been interesting to study higher values of q for which

TABLE III. Three-state Potts model: the symmetries of a periodic chain combined with the S_3 color symmetry. Same notations as in Table I, but C has three possible values $C=0, 1$, or 2 . There is an extra twofold degeneracy for $C=2$.

Three-state Potts model on a periodic square lattice							
$N=11$ dim=177 147							
R	k	λ	l_R	$a_{R,C=0}$	$a_{R,C=1}$	$a_{R,C=2}$	a_R
0	0	1	1	1464	1342	2806	8418
1	π	-1	1	1221	1342	2563	7689
2	$\pi/11$	*	2	2684	2684	5368	16104
3	$2\pi/11$	*	2	2684	2684	5368	16104
4	$3\pi/11$	*	2	2684	2684	5368	16104
5	$4\pi/11$	*	2	2684	2684	5368	16104
6	$5\pi/11$	*	2	2684	2684	5368	16104

the transition becomes first order, but the size of the transfer matrix is an exponential function of the number of states q , and values of q larger than 3 lead to extremely large matrices even for a small lattice size. The transfer matrix T has the same form [Eq. (11)] as for the two-dimensional Ising model in absence of magnetic field. The matrix $V(K_2)$ is a $3^N \times 3^N$ diagonal matrix with entries

$$[V(K_2)]_{i,j} = \prod_{i=0}^{N-1} w_2^{\delta(\alpha_i, \alpha_{i+1})}, \quad (19)$$

where $\alpha_i = 0, 1$ or 2 is the value of the i th spins in the spin configuration labeled α . The matrix $H(K_1)$ is a symmetric matrix

$$H(K_1) = h(K_1)^{\otimes N}, \quad h(K_1) = \begin{pmatrix} w_1 & 1 & 1 \\ 1 & w_1 & 1 \\ 1 & 1 & w_1 \end{pmatrix}. \quad (20)$$

The space symmetry group is \mathcal{D}_N as in the case of the Ising model, but the color symmetry group is S_3 rather than S_2 for the Ising model. The size reduction is better in the Potts case, but far less than the exponential increase, due to the three states. Table III gives the size of the blocks in the different invariant subspaces. In Fig. 6 we present two typical level spacing distributions. The upper one (a) is obtained at the critical value of the Boltzmann weight $w^* = 1 + \sqrt{3}$, and the other one is obtained at a different value $w = 1.4$ far from the transition. It is obvious that at w^* the distribution is very close to an exponential, while for $w \neq w^*$ this distribution is close to the Wigner surmise. Figure 7 shows the rigidity Δ_3 for the same values of the Boltzmann weights. We observe the same coincidence with the theoretical behavior expected for independent numbers and spectra of GOE matrices. The agreement with the GOE behavior extends up to a value $L \approx 4$. This value is much less than for the two-dimensional Ising model in a field, but is comparable with values obtained in some quantum models [14]. In Fig. 8 we present the behavior of the best fitted value β of the parametrized distribution as a function of temperature. Several sizes $N = 8, 9, 10$, and 11 are plotted. We first note that the

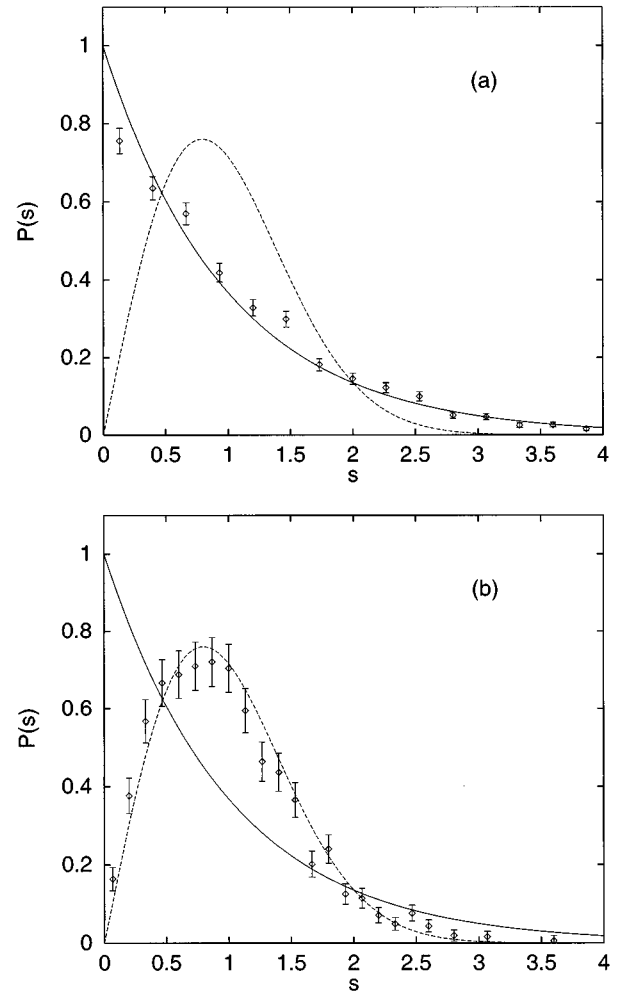


FIG. 6. Eigenvalue spacing distribution for the three-state Potts model (a) precisely at the critical point $w_1 = w_2 = 1 + \sqrt{3}$, and (b) far from the critical point at $w_1 = w_2 = 1.4$. The data are obtained for $N=11$ and the number of spacings are 2500 (a) and 1400 (b).

spacing distribution has properly ‘‘detected’’ the integrable point w^* , which corresponds precisely to the minimum in the $\beta(w)$ curve. We also observe size effects: for larger size the downward peak is sharper than for smaller size. This

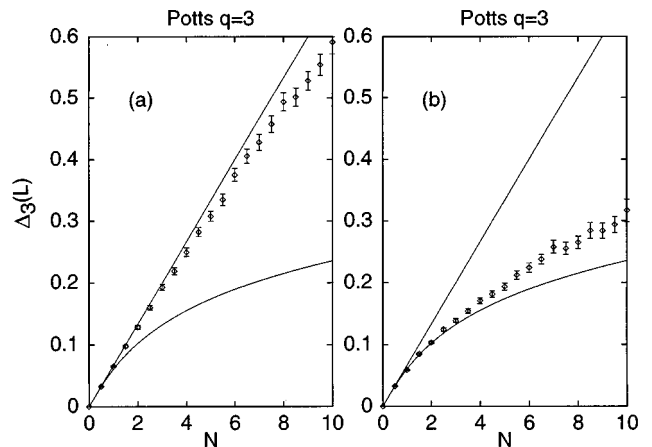


FIG. 7. The rigidity $\Delta_3(L)$ for the same parameters as in Fig. 6.

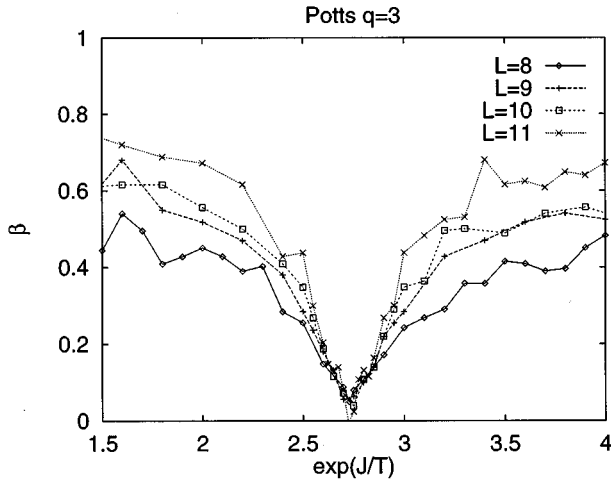


FIG. 8. The parameter β as a function of the temperature for a three-state Potts model for different lattice sizes. The minimum is at the critical point which is integrable.

suggests that in the thermodynamic limit the spacing distribution is a Poisson law *only* at the critical temperature.

We again found that integrability leads to independent eigenvalues, whereas nonintegrability leads to eigenvalue repulsion properly described by the spectral statistical properties of the GOE: the analysis of the statistical properties of the spectrum of the transfer matrix can be used to find integrable points.

E. Three-state Potts model for negative Boltzmann weights

We now look at the isotropic three-state Potts model with $w < 0$. The transfer matrix is still symmetric, but some entries become imaginary, since we have half-integer powers of negative numbers [see Eqs. (19) and (11)]. We numerically found that the spectrum is complex only when $-2 < w < 0$. Thus when $w < -2$ one can apply the standard RMT analysis. We have found a GOE spacing distribution as expected. When $-2 < w < 0$ the spectrum contains mostly complex conjugate eigenvalues. By spacing we now mean the shortest Euclidian distance between eigenvalues in the complex plane, and we use another unfolding procedure (Ref. [4], Chap. 8.6). We want to know if the unfolded eigenvalues are “independent” or if they repel each other. The spacing distribution of independent points in d dimensions is easy to evaluate: for N points taken randomly on a d -dimensional hypersphere of radius $N^{1/d}$, the probability that the distance between a point and its closest neighbor is s , is the probability that exactly one point is found at the distance between s and $s+ds$, and that the other $N-2$ points are farther away than s :

$$P_N(s)ds \propto s^{d-1} \left[1 - \left(\frac{s}{N^{1/d}} \right)^d \right]^{(N-2)} ds. \quad (21)$$

Taking the limit $N \rightarrow \infty$, one obtains $P(s) \propto s^{d-1} \exp(-Cs^d)$ (C is some constant). For $d=2$ one recovers precisely the Wigner law which is a well known distribution in mathematical statistics. In other words a Wigner law for a one-dimensional set of points means repulsion between these points, whereas for points in the plane the same Wigner law

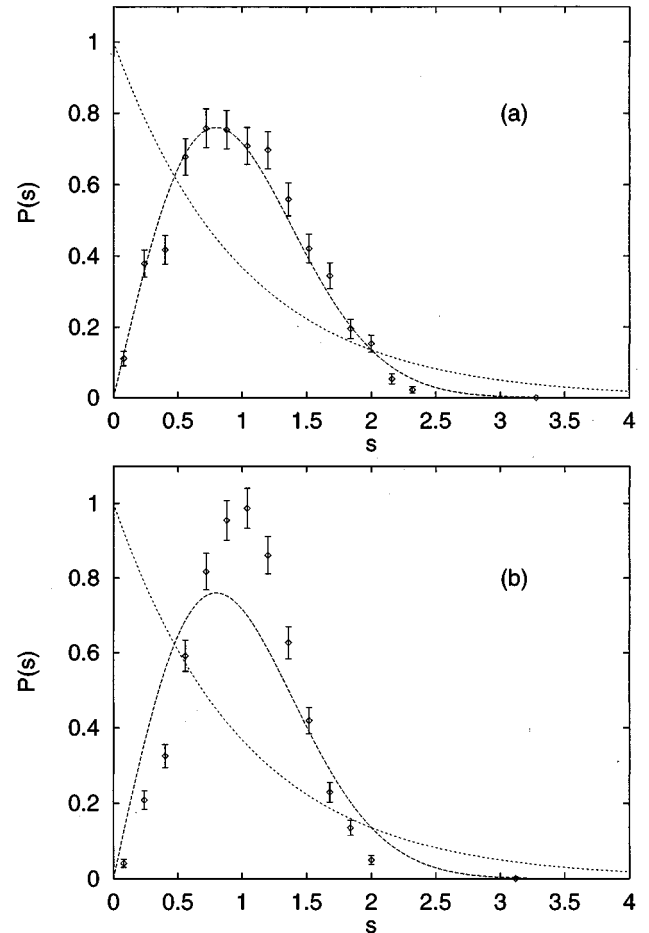


FIG. 9. Two closest-distance distributions for the isotropic three-state Potts model with negative Boltzmann weight: (a) for the self-dual Boltzmann weight $w_1 = w_2 = w_{SD} = 1 - \sqrt{3}$, and (b) for a different value $w_1 = w_2 = -1.5$. The average runs over about 2000 spacings.

means independence. The probability that random points in the plane are close to each other is already small, and a supplementary repulsion due to correlations of nonintegrability will have less influence than in the case of a real spectrum. For nonsymmetric random matrices the joint probability distribution of the eigenvalues was studied [23]. Eigenvalue repulsion is still present, but a closed expression for the degree of repulsion is not known.

In Fig. 9(b) we present a distribution of eigenvalue spacings for $w = -1.5$: the repulsion is clearly seen, since $P(s)$ near the origin is smaller than for the Wigner law. We note that this distribution is not close to the eigenvalue spacing distribution of the spectra of another universal ensemble GUE or GSE. We also have investigated another special point in the regime $-2 < w < 0$. The self-duality equation $(w_{SD} - 1)^2 = q$ has a solution $w_{SD} = 1 - \sqrt{3}$ which lies in this regime. In Fig. 9(a) we present the distribution of eigenvalue spacings at this value $w_{SD} = 1 - \sqrt{3}$. The agreement with the Wigner law, which here means independence, is quite good. This is expected since the point w_{SD} is also integrable.

IV. DISCUSSION AND CONCLUSION

We showed numerically that the eigenvalues of the transfer matrix of an integrable spin model have many features of

random independent numbers. Conversely, the spectrum of the transfer matrix of a nonintegrable spin model has many features in common with the spectrum of a GOE matrix. In particular, the spacing distribution is an exponential law for integrable systems, while it is close to the Wigner surmise for nonintegrable systems. Quantities involving more than two closest eigenvalues, like the rigidity, also show a GOE behavior on quite a large scale involving up to 25 eigenvalues in the case of the square lattice Ising model with field. The independence of eigenvalues for integrable models has been checked on the Ising model in two dimensions in the absence of a magnetic field, as well as on the critical point of the three-state Potts model. We also have studied the transition point of a three-dimensional Ising model, for which we have found eigenvalue repulsion and a good agreement of the spacing distribution with the Wigner surmise. This stresses the difference between criticality and integrability: the eigenvalue statistics is sensible to integrability and not to criticality.

Using the eigenvalue statistics as a criterion of integrability, we support the hypothesis that the two-dimensional Ising model in a field and the three-dimensional Ising model are not integrable. The integrable models appear as very singular and isolated in parameter space. This is clearly seen in curves showing the parameter β as a function of a Boltzmann weight, where β is close to unity almost everywhere, except for the particular values where the model is integrable. With the sizes numerically tractable, the variation of β is abrupt, and the size behavior suggests that in the thermodynamic limit the statistics changes discontinuously. To clarify this point, a more detailed study of the size effects is needed. It would also be interesting, but difficult, to study the Potts model with a large number of states to have a first order phase transition point which is integrable.

To use the criterion of eigenvalue spacing statistics with new models (for example, chiral models) one needs to study complex spectra in many cases. The distinction between independent eigenvalues for integrable models and repelling eigenvalues for nonintegrable models still holds. However, a repulsion between eigenvalues in one dimension is much easier to quantify than in two dimensions. Intuitively this can be understood since in two dimensions the eigenvalues are not restricted to a line and have naturally more space to avoid each other. The repulsion between eigenvalues in two dimensions has less effect than in one dimension. We have found that for the three-state Potts model and for a Boltzmann weight $-2 < w < 0$ the spectrum is complex, and that the eigenvalue spacing distribution is characteristic of eigenvalue repulsion. However, when w is close to the negative self-dual value, we recover a distribution close to the Wigner law indicating here an eigenvalue independence associated with integrability. The numerical difficulties arising from complex spectra are of importance, and we need to refine further the analysis, and especially the unfolding, to study convincingly chiral models. This is in progress.

In these two papers we showed numerically that the statistical properties of transfer matrix spectra of classical statistical mechanics models are related to the integrability of the model, extending hereby the field of application of RMT. This can be useful in the search for new integrable models.

ACKNOWLEDGMENT

We thank J.-M. Maillard for many discussions, where his expertise with integrable models has been very precious.

APPENDIX A

It was established in [19] that the spectrum of the row-to-row anisotropic Ising model for an even size N is given by

$$\Lambda_\tau(K_1, K_2) = [2 \sinh(2K_1)]^{N/2} \exp\left(-\frac{1}{2} \sum_{q=0}^{N-1} \tau_q \epsilon_q\right), \tag{A1}$$

where $\tau_q = \pm 1$ according to the q th digit of the binary representation of τ ($0 \leq \tau < 2^N$), and, for all q with $0 \leq q < N$,

$$\cosh \epsilon_q = \cosh 2K_2 \cosh 2K_1^* - \sinh 2K_2 \sinh 2K_1^* \cos Q, \tag{A2}$$

where $Q = (2q + 1)\pi/N$ if there is an even number of 1 in the base two representation of τ , and $Q = 2q\pi/N$ otherwise. For ϵ_q , the positive root of Eq. (A2) has to be taken except for $Q = 0$, where $\epsilon_0 = 2(K_1^* - K_2)$ and for $Q = \pi$ where $\epsilon_{N/2} = 2(K_1^* + K_2)$. K_1^* is the dual coupling constant defined by $\tanh K_1 = e^{-2K_1^*}$. The derivative of $\Lambda_\tau(K_1, K_2)$ with respect to K_2 is

$$\frac{\partial \Lambda_\tau(K_1, K_2)}{\partial K_2} = -\frac{1}{2} \Lambda_\tau(K_1, K_2) \sum_{q=0}^{N-1} \tau_q \frac{\partial \epsilon_q}{\partial K_2}, \tag{A3}$$

with

$$\frac{\partial \epsilon_q}{\partial K_2} = 2 \frac{\sinh 2K_2 \cosh 2K_1^* - \cosh 2K_2 \sinh 2K_1^* \cos Q}{\sinh \epsilon_q}. \tag{A4}$$

It is easy to check that, for an *even* number of particles,

$$\epsilon_q = \epsilon_{N-1-q} \quad \text{and} \quad \frac{\partial \epsilon_q}{\partial K_2} = \frac{\partial \epsilon_{N-1-q}}{\partial K_2} \quad (0 \leq q < N/2), \tag{A5}$$

while, for an *odd* number of particles,

$$\epsilon_q = \epsilon_{N-q} \quad \text{and} \quad \frac{\partial \epsilon_q}{\partial K_2} = \frac{\partial \epsilon_{N-q}}{\partial K_2} \quad (1 \leq q < N/2) \tag{A6}$$

and

$$\epsilon_0 = 2(K_1^* - K_2), \quad \frac{\partial \epsilon_0}{\partial K_2} = 2, \tag{A7}$$

$$\epsilon_{N/2} = 2(K_1^* + K_2), \quad \frac{\partial \epsilon_{N/2}}{\partial K_2} = -2. \tag{A8}$$

When the size N is a multiple of 4 and when there are $N/2$ particles, then the number of particles is even, and we must use formula (A5). There are $2^{N/2}$ choices of τ such that $\tau_q = -\tau_{N-1-q}$ for $0 \leq q < N/2$. In that case one has

$$\sum_{q=0}^{N-1} \tau_q \frac{\partial \epsilon_q}{\partial K_2} = \sum_{q=0}^{N/2-1} (\tau_q - \tau_{N-1-q}) \frac{\partial \epsilon_q}{\partial K_2} = 0. \tag{A9}$$

This gives $2^{N/2}$ K_2 -independent states.

N being still a multiple of 4 and taking $N/2 \pm 1$ particles, we now must use formulas (A6) and (A7). There are $2 \times 2^{N/2-1}$ choices of τ such that $\tau_q = -\tau_{N-q}$ for $1 \leq q < N/2$ and $\tau_0 = \tau_{N/2}$. In that case one has

$$\sum_{q=0}^{N-1} \tau_q \frac{\partial \epsilon_q}{\partial K_2} = \pm (\epsilon_0 + \epsilon_{N/2}) + \sum_{q=1}^{N/2-1} (\tau_q - \tau_{N-1-q}) \frac{\partial \epsilon_q}{\partial K_2} = 0 \quad . \quad (\text{A10})$$

Collecting the three cases mentioned above, we obtain $2^{N/2+1}$ K_2 -independent states. It is then simple to verify that the corresponding eigenvalues are

$$2^N (\sinh K_1)^p (\cosh K_2)^{N-p} \quad , \quad (\text{A11})$$

where $p = N/2 - 1$, and $N/2$ or $N/2 + 1$ is the number of particles.

-
- [1] H. Meyer, J.-C. Anglès d'Auriac, and H. Bruus, *J. Phys. A* **29**, L483 (1996).
- [2] H. Meyer, J.-C. Anglès d'Auriac, and J.-M. Maillard, *Phys. Rev. E* **55**, 5261 (1997).
- [3] M. C. Gutzwiller, *Chaos in Classical and Quantum Mechanics* (Springer, New York, 1990).
- [4] F. Haake, *Quantum Signatures of Chaos* (Springer, Berlin, 1991).
- [5] R. Baxter, *Phys. Rev. Lett.* **26**, 832 (1971); *Ann. Phys.* **70**, 193 (1972).
- [6] R. Baxter, *Exactly Solved Models in Statistical Mechanics* (Academic, New York, 1982).
- [7] G. H. Wannier, *Rev. Mod. Phys.* **17**, 50 (1945).
- [8] E. H. Lieb and F. Y. Wu, in *Phase Transitions and Critical Phenomena*, edited by C. Domb and M. Green (Academic, New York, 1972), Vol. 1, pp. 331–490.
- [9] M. L. Mehta, *Random Matrices*, 2nd ed. (Academic, San Diego, 1991).
- [10] D. Poilblanc, T. Ziman, J. Bellisard, F. Mila, and G. Montambaux, *Europhys. Lett.* **22**, 537 (1993).
- [11] T. C. Hsu and J.-C. Anglès d'Auriac, *Phys. Rev. B* **47**, 14291 (1993).
- [12] G. Montambaux, D. Poilblanc, J. Bellisard, and C. Sire, *Phys. Rev. Lett.* **70**, 497 (1993).
- [13] P. van Ede van der Pals and P. Gaspard, *Phys. Rev. E* **49**, 79 (1994).
- [14] H. Bruus and J.-C. Anglès d'Auriac, *Europhys. Lett.* **35**, 321 (1996).
- [15] H. Bruus and J.-C. Anglès d'Auriac, *Phys. Rev. B* **55**, 9142 (1997).
- [16] On the transfer matrix see, for example, [17,7,6] or any textbook on statistical mechanics.
- [17] H. A. Kramers and G. H. Wannier, *Phys. Rev.* **60**, 252 (1941).
- [18] L. Onsager, *Phys. Rev.* **65**, 117 (1944).
- [19] T. D. Schultz, D. C. Mattis, and E. H. Lieb, *Rev. Mod. Phys.* **36**, 856 (1964).
- [20] C. Itzykson, *Nucl. Phys. B* **210**, 477 (1982).
- [21] F. Y. Wu, *Rev. Mod. Phys.* **54**, 235 (1982).
- [22] R. B. Potts, *Proc. Cambridge Philos. Soc.* **48**, 106 (1952).
- [23] N. Lehmann and H.-J. Sommers, *Phys. Rev. Lett.* **67**, 941 (1991).